



Intensification of isoamyl acetate production: transport properties of silica membranes

Wilmar Osorio-Viana^a, Jesús-David Quintero-Arias^a, Izabela Dobrosz-Gómez^b
Javier Fontalvo^a, Miguel Angel Gómez-García^{a,*}

^a*Departamento de Ingeniería Química, Facultad de Ingeniería y Arquitectura, Universidad Nacional de Colombia—Sede Manizales, Grupo de Investigación en Aplicación de Nuevas Tecnologías, Laboratorio de Intensificación de Procesos y Sistemas Híbridos, Cra 27 No. 64-60, Manizales, Apartado Aéreo 127, Colombia Tel. +57 6 887 93 00 (50210); Fax: +57 6 887 93 00 (50129); email: magomez@unal.edu.co*

^b*Departamento de Física y Química, Facultad de Ciencias Exactas y Naturales, Universidad Nacional de Colombia—Sede Manizales, Grupo de Investigación en Aplicación de Nuevas Tecnologías, Laboratorio de Intensificación de Procesos y Sistemas Híbridos, Cra 27 No. 64-60, Manizales, Apartado Aéreo 127, Colombia*

Received 25 November 2011; Accepted 6 March 2012

ABSTRACT

Fuel ethanol production by fermentation generates isoamyl alcohol as by-product. Its conversion to isoamyl acetate is an alternative to obtain a higher value product. An intensified reaction–pervaporation process is an attractive option compared to conventional distillation. The design of this process requires the characterization of the transport properties of the membrane used. Xerogel type ceramic membranes were prepared by dip-coating and analyzed by using Brunauer-Emmett-Teller method, fourier transform infrared spectroscopy, and scanning electron microscopy–energy dispersive spectrometer methods. Their hydrophilic and microporous character was confirmed. Using quaternary mixtures of the esterification process, a membrane was evaluated for water separation in a laboratory scale pervaporation unit. A special experimental protocol for membrane evaluation was proposed for the multi-component reactive mixture. Experimental membrane flux and selectivity were determined and used to correlate three basic mass transport models. Among them, the most suitable and reliable was the thermodynamic Fick model, which can be used for reaction-pervaporation process design and simulation.

Keywords: Isoamyl acetate; Silica membranes; Pervaporation; Membrane mass transport models

1. Introduction

During the last few years, the production of ethanol by fermentation has been increased considerably

in Colombia due to the governmental policy, as stated by the laws 693 of 19 September 2001 and 1135 of 31 March 2009 of Ministry of Mines and Energy [1]. Alcoholic fermentation is not a completely selective process to ethanol production and fusel oil is formed as a by-product. Isoamyl alcohol, with a mass fraction close to 75 wt.% in water-free base, is the main component of fusel oil [2]. Recently, a strong interest

*Corresponding author.

for isoamyl alcohol industrial exploitation as a raw material for isoamyl acetate production by esterification of acetic acid has been observed [3,4]. This liquid phase reaction is represented by Eq. (1).



This reaction is equilibrium limited due to its low equilibrium constant ($K_{\text{eq}} \approx 5$) [5,6]. Separation of the acetic acid/isoamyl alcohol/isoamyl acetate/water esterification mixture can be accomplished by conventional distillation, reactive distillation, or pervaporation (a membrane technology). From a thermodynamic point of view, the removal of water from the reactive mixture by pervaporation, instead of ester removal, can reduce separation efforts and process complexity. This is because water causes mixture nonidealities as phase segregation [7,8]. Pervaporation is considered as a technological alternative for simultaneous reaction-separation process with energy consumption lower than the conventional distillation [9,10]. The choice of membrane for pervaporation should be made according to its affinity to a key component. In fact, the use of hydrophilic membranes for separation can prove a yield increase in the equilibrium limited reaction conversion of 70–75% [11]. Two kinds of membranes can be considered for the application discussed: ceramic and polymeric. In general, ceramic membranes present better thermal, chemical, and mechanical stability compared to polymeric membranes. Considering that membrane equipment cost is directly proportional to its area, the ideal one should achieve the required separation with a minimum area [12]. Therefore, membrane performance influences the technical viability and economics of the hybrid membrane esterification reactor. In this work, an easy prepared low cost silica tubular membrane with large surface area is used.

Experimental pervaporation studies for esterification systems should consider membrane process productivity, separation capacity, and stabilization time of the membrane. However, several drawbacks exist in conventional pervaporation test. Usually, in batch pervaporation experiments an appropriate relationship between membrane area and liquid retentate mixture volume is set. This allows to render negligible the changes in the retentate composition during the experiment. The experiment is carried out at isothermal conditions in each run with fixed retentate composition, measuring the corresponding membrane stable flux [16]. Constant retentate composition is easy to reach for single or binary nonreactive mixtures. A negligible variation of flux over time is considered as

the membrane stabilization criterion [17]. Based on typical flux data (1–5 kg/m² h for pervaporation experiments with ceramic membranes), the required amount of liquid retentate (M_o) is calculated by using Eq. (2), considering that composition changes in the mixture are less than 5%.

$$M_o = \frac{\text{Removed mass}}{\text{Permissible percentage change} \times \text{Initial water mass fraction}} \quad (2)$$

Thus, in many cases, with a conventional experiment the required liquid volume is very high. Additionally, if a reactive liquid mixture is used, the composition in the liquid will change with time because of both: the pervaporation and the reaction processes. Consequently, pervaporation experiments for esterification membrane reactors are usually performed close to equilibrium conditions of the reactive mixture. However, the hybrid pervaporation–esterification reactor operates far from equilibrium conditions [18–20]. Extrapolation of “equilibrium” experimental results to other distant operating conditions is not desirable considering that permeance is not constant and highly depends on composition. Consequently, a new method for pervaporation test was devised in this work.

The definition of a transport model completes the membrane characterization for processes design. In fact, an approximate relationship between flux and concentration is required. Then, experimental data must be correlated to a chosen transport model. It should be able to predict operating condition parameters, while being precise and simple enough for process simulation. However, transport models can differ in complexity according to process features [13–15]. The flux in pervaporation processes can be described by the following expression [15]:

$$N_i = \frac{P_{M_i}}{L_M} (\gamma_i x_i P_i^s - y_i P) \quad (3)$$

where N_i is the flux, P_{M_i} is the permeability, L_M is the membrane thickness, γ_i is the activity coefficient of the substance i , x_i is the molar fraction in retentate, P_i^s is the vapor pressure, y_i is the molar fraction in permeate, and P is the permeate total pressure. Neglecting $y_i P$, because working pressures are usually low (3–5 mbar), Eq. (3) reduces to:

$$N_i = \left(\frac{P_{M_i} \gamma_i P_i^s}{L_M} \right) x_i \quad (4)$$

Then, several mass transport models can be used for flux data correlation. Fick and solution-diffusion type models were used in this work.

Here the synthesis, characterization, and performance of a tubular hydrophilic silica membrane for water removal by pervaporation of acetic acid, isoamyl alcohol, isoamyl acetate, and water mixtures are presented. An alternative experimental method is also proposed. Experimental data were fitted to a suitable permeation model.

2. Experimental

2.1. Membrane preparation and characterization

Hollow fibers (Hyflux CEPAration-Netherlands) ceramic membranes with length of 30 cm, an inner and outer diameter of 2.0 and 3.0 mm, respectively, and pore size of 200 nm were used as a support. Three intermediate layers of γ -alumina and, on top of it, three layers of silica were deposited by dip-coating at room temperature in a cupboard to minimize dust contamination. Corresponding γ -alumina and silica layers were deposited using boehmite and silica gel solutions, respectively.

Boehmite (γ -AlOOH) sol was synthesized according to the procedure presented by Peters et al. [17]. Dip-coating velocity of 3.3 cm s^{-1} was used in boehmite solution deposition to obtain a layer thickness of ca. $4 \mu\text{m}$ [21–23]. Subsequently, each alumina layer was dried at 40°C for 2 h and calcined at 600°C for 3 h, with a ramp rate of 1°C min^{-1} .

Hydrophilic silica gel was prepared by acid catalyzed (HNO_3) sol-gel method, using the following molar ratio TEOS (1):ethanol (3,8):water (6,4):nitric acid (0.085) [14,15]. The synthesis was based on the hydrolysis and subsequent polycondensation of tetraethyl-orthosilicate (TEOS) (Merck, purity > 99%) dissolved in ethanol (Merck, purity > 99.9%). The final density and viscosity of the obtained silica gel was 0.79 g cm^{-3} and 1.29 cP , respectively. As synthesized gel was divided in two parts, one part was used for silica membranes deposition and another one was kept as prepared for characterization (here there after powder silica xerogel). Dip-coating velocity of 1.0 cm s^{-1} was used in silica gel deposition. Each deposited silica layer was dried at 40°C for 30 min and calcined in air, (at 400°C), for 4 h, with a ramp rate $0.5^\circ\text{C min}^{-1}$.

The specific surface area, pore volume, pore size, and their distribution were measured for powder silica xerogels (gel without dissolution in ethanol) by N_2 -physisorption at liquid nitrogen temperature using a Gemini 2360 (Micromeritics, Germany) surface area analyzer. Prior to the measurement, the samples were degassed for 480 min at 200°C . The specific surface area was calculated according to the Brunauer-Emmett-Teller model, while the pore size distribution and the

pore volume were calculated using the Horvath and Kawazoe (HK) method for microporous materials.

The fourier transform infrared spectroscopy (FTIR) characterization of powder silica xerogel was performed in a Nicolet 6700 FTIR spectrometer (Thermo Scientific, USA) with MCT detector (photoconductive detector HgCdTe) using a standard sample holder. Transmittance measurements were performed using KBr technique. Pellets were prepared with 5 wt.% of silica and 95 wt.% of potassium bromide (KBr) pressed at 1,800 psi for 5 min. The FTIR spectra were recorded in the mid-infrared range of $4,000\text{--}400 \text{ cm}^{-1}$ at room temperature.

Morphological studies of silica and alumina membranes were performed using a S-4700 scanning electron microscopy (SEM, Hitachi, Japan) coupled with energy dispersive spectrometer (EDS, Thermo Noran, USA) at an acceleration voltage of 25 kV. For these studies, membranes were cut into cylinders of 1.5 cm length. The SEM and EDS studies were carried out in the cylinder's cross and lateral sections, respectively. The examined samples were placed on carbon plasters in a holder and before analyzing were coated with a carbon monolayer using Cressington 208 HR system (Cressington Scientific Instruments Ltd., UK), in order to reduce the charge build-up on the samples.

2.2. Pervaporation experimental design and setup

Membrane transport properties like flux, selectivity, pervaporation separation index (PSI), diffusivity, and stability time should be determined at operating conditions similar to those that will be found in the industrial applications [25,26]. In this work, experiments were performed for mixtures of acetic acid/isoamyl alcohol/isoamyl acetate/water. The concentration of the mixture depends on membrane and reactor configuration, either *in situ* or *ex situ* [7,9]. In the first case, the membrane will be operating with a reactive mixture at intermediate conversions, while in the second case with mixtures near chemical equilibrium. Therefore, experiments were carried out using mixtures with compositions equivalent to those expected in a reactor loaded with stoichiometric amounts of isoamyl alcohol and acetic acid in the conversion range of 10–75% (Table 1).

A typical setup was used for pervaporation [25], as shown in Fig. 1. A 2 L jacket vessel, with controlled temperature by a thermostatic bath, containing a liquid mixture (retentate) was used. Inside of it one tubular membrane was submerged. On the permeate, side vacuum was maintained (3–5 mbar) by a pump connected to the internal part of the membrane. Vapor

Table 1
Mixture mass composition and temperature ranges used in pervaporation experiments

Compound	Acetic acid	Isoamyl alcohol	Isoamyl acetate	Water	Temperature (°C)
Mass fraction	0.3647–0.0608	0.5353–0.0892	0.0878–0.7467	0.0122–0.1033	40–60

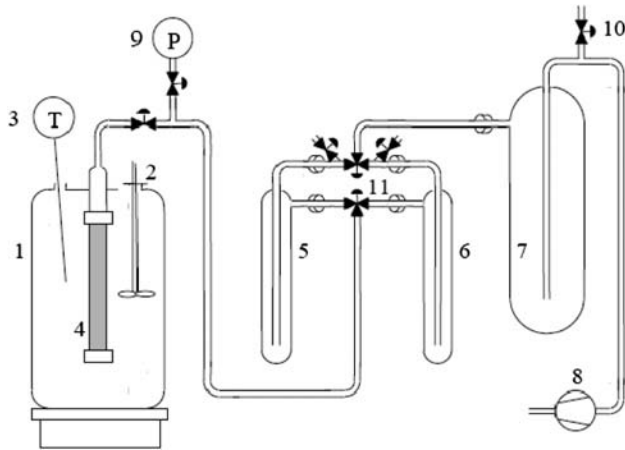


Fig. 1. Laboratory scale experimental setup for pervaporation process. (1) Glass vessel with heating jacket; (2) stirrer; (3) temperature probe; (4) membrane; (5) and (6) permeate sample collectors; (7) cold trap; (8) vacuum pump; (9) pressure sensor; (10) pressure controller; (11) valve to control glass collector admission.

permeates through the membrane and passes to a cascade of liquid nitrogen cold traps to condense. At regular time intervals, the retentate and permeate samples were collected to quantify their mass and composition. The mass of permeate collected divided by membrane area and sampling time gives the total flux at experimental conditions. In practice, some time is required to obtain stable flux values in the equipment. This stabilization time depends on membrane material, mixture nature, and composition and pervaporation operational conditions.

Experimental results for pervaporation experiments at temperatures of 40, 50, and 60°C and retentate water concentrations of 4–10 wt.% are presented. Pure chemicals were used in the experiments without further treatment. Samples were analyzed by gas chromatography (Perkin Elmer Autosystem XL with FID detector) and Karl Fischer titration (Metrohm 702 SM titrino).

2.3. Pervaporation test

For conditions presented in Table 1, retentate mass varies in the range of 0.493–2.46 kg/h, in the best case

scenario, and between 4,170 and 20,852 kg/h for the extreme case of low concentration. Taking into account that pervaporation experiments last between 6 and 12 h, it is easily concluded that with this conventional experiment the required liquid volume is high. If a reactive liquid mixture is used, compositions change with time because of the pervaporation process and the reaction that take place simultaneously in the liquid. Then, a new experimental procedure was designed as follows. In an experiment, at a given temperature, the aggregation of terms $((P_{M_i} \cdot \gamma_i \cdot P_i^s) / LM)$, in Eq. (4), can be considered constant within small compositions ranges. This means a linear relationship between flux and retentate concentration at steady state. Considering that it is easier to handle mass fraction compositions, it was proposed a linear relationship between flux and retentate mass fraction for each substance in the mixture at steady state within a small range of retentate concentrations (as suggested by Wesslein et al. [27]). Consequently, when flux is plotted vs. retentate composition during the time of an experimental run, two zones will be distinguished in such plot: a high flux and nonconstant slope zone (unstable operation zone) and a second zone when the slope remains constant (stable operation zone). Stable operation zone provides the required values of membrane flux. Several mass transfer models can be applied to describe the permeation phenomenon occurring during pervaporation. As a preliminary attempt, Fick and solution-diffusion type models are used to fit experimental data due to its simplicity and low number of adjustable parameters. More rigorous models for multicomponent mass transfer like Maxwell–Stefan or dusty-gas model will be treated in a related upcoming publication.

The classic expression of Fick's law is given by Eqs. (5) and (6):

$$N_i = -c_t D_{ij} \frac{dx_i}{dl} \quad (5)$$

$$D_{ij} = D_{ij_0} \times e^{-\frac{E_a}{RT}} \quad (6)$$

where c_t is the total concentration, D_{ij} is the diffusivity, and dx/dl is the change in the mole fraction with

membrane thickness. This expression is frequently used for binary systems and, using empirical methods, it has been extended to multicomponent systems. Through standard thermodynamic relations [28,29], Eq. (5) can be manipulated to obtain:

$$N_i = -c_i D_{ij} \frac{d \ln(a_i)}{dl} \quad (7)$$

where c_i is the concentration of component i , R is the universal gases constant, T is the temperature in Kelvin, μ is the chemical potential, and a_i is the chemical activity.

Solution-diffusion model assumes that pervaporation process occurs by mass transfer through the membrane due to fugacity difference between retentate (liquid) and permeate (vapor) phases, according to Eq. (8) [15]:

$$N_i = \frac{P_{M_i}}{L_M} (x_i \gamma_i f_i - y_i \phi_i P) \quad (8)$$

where f_i stands for liquid fugacity and ϕ_i is the vapor fugacity coefficient (both calculated with the Hayden–O'Connell model to account for acetic acid dimerization). In order to correlate a permeation model, experimental data were treated as follows:

- Discrimination of stable data:* every retentate and permeate sample during the pervaporation experiment is used to measure the flux and the composition of every component, for triplicate. With these three measurements, the mean value and standard deviation is calculated. Then, the mean value of flux for each component (total flux times mass fraction) vs. time is plotted. This plot is used to identify a zone of stable slope corresponding to the stable pervaporation regime. The data in the stable zone are the only data used for further processing.
- Linear regressions:* the data in the stable zone undergo a linear regression analysis. Mean value of flux for each component vs. retentate mass fraction is plotted and the respective linear regression is performed. The equations obtained with the aid of the linear regression analysis are used to generate simulated data of flux vs. concentration for the correlation of the permeation models.
- Model correlation:* for a specific permeation model, a nonlinear regression analysis is performed using an optimization numerical method to obtain the values of its adjustable

parameters [30,31]. Minimum least squares type objective between experimental and calculated values for the flux is used for the optimization problem. MatLab[®] function *nonlinearfit* was used for the computations. Convergence to a global minimum was verified using different initial values. Analysis of residuals must show a random distribution with mean zero and constant standard deviation.

3. Results and discussion

3.1. Membrane textural and surface characterization

The hydrophilic nature of silica is attributed to the presence of hydroxyl groups (–OH) on silica surface, evidenced as broad bands at $3,748 \text{ cm}^{-1}$ and $3,400\text{--}3,500 \text{ cm}^{-1}$ at FTIR silica spectrum (Fig. 2). This characteristic bands can be related to the presence of groups (Si–OH) and O–H stretching bands which are caused by hydrogen-bonded water molecules (H–O–H ··· H) and, surface silanol groups, hydrogen-bonded to the molecular water (Si–O–H...H₂O) [24]. Moreover, the hydrophilic nature of the silica xerogel can be evidenced by the $1,640 \text{ cm}^{-1}$ band (Fig. 2), corresponding to the water vibration adsorbed on silica surface as well as at 960 cm^{-1} , assigned to Si–O in plane stretching vibrations of the silanol (Si–OH) group. The other characteristic bands observed in the range of $1,200\text{--}1,000 \text{ cm}^{-1}$ and at 800 cm^{-1} are related to the antisymmetric and symmetric vibrations of Si–O–Si with minima at $1,076 \text{ cm}^{-1}$ and 801 cm^{-1} , respectively. The vibration mode appearing at $1,231 \text{ cm}^{-1}$ can be assigned to the symmetric deformation of C–H in CH₂ groups, corresponding to residual nonhydrolyzed alkoxy groups (–OC₂H₅) on the silica xerogel surface. Table 2 shows characteristic vibration frequencies in FTIR spectra of hydrophilic silica xerogel.

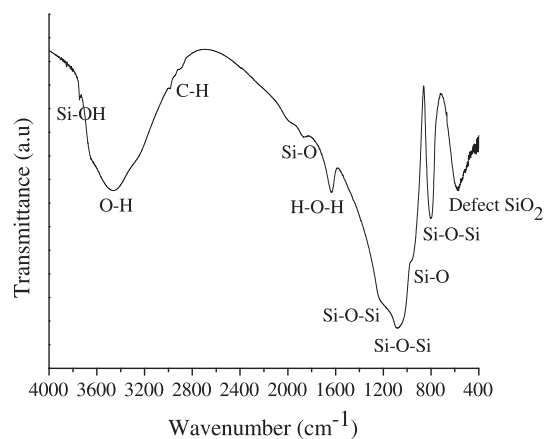


Fig. 2. FTIR spectrum of prepared silica xerogel.

Table 2
Characteristic vibration frequencies in FTIR spectra of hydrophilic silica xerogel (adapted from [32])

Wavenumber (cm ⁻¹)	Vibration type	Structural unit	Reference
3,740	Si–OH	Si–OH...H ₂ O	[33]
3,664–2,966	O–H	H–O–H...H ₂ O	[34]
2,927	ν_{as} C–H	CH ₂	[34]
2,856	ν_s C–H	CH ₂	[34]
2,364	C=O	CO ₂	[35]
1,860	C=O	Carbonyl groups	[35]
1,640	δ H–O–H	H ₂ O	[34]
1,588	C=O	Carbonyl groups	[35,36]
1,526	C–H	Si–C ₂ H ₅	[35]
1,270–690	ν_{as} Si–O–Si	Si–O–Si	[34,35]

δ : deformation vibration, ν_{as} : antisymmetric stretching vibration, and ν_s : symmetric stretching vibration.

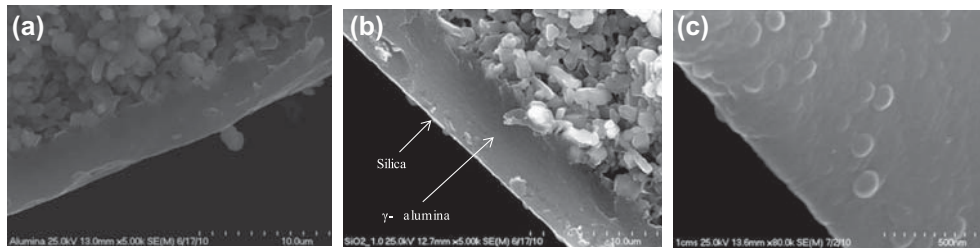


Fig. 3. SEM micrographs of: (a) cross-section of the intermediate γ -alumina layers deposited on the top of tubular ceramic membrane support (magnifications 5,000 \times) and (b) and (c) cross-section of hydrophilic silica membrane deposited with dip-coating velocity of 1 cm s⁻¹ on the intermediate γ -alumina layers (magnifications 5,000 \times and 80,000 \times , respectively).

Fig. 3 presents a typical cross-section of intermediate γ -alumina layers deposited on the top of the tubular ceramic membrane support (Fig. 3a). Moreover, three deposited γ -alumina layers form a single homogeneous layer with thickness of ca. 4 μ m, estimated with the MeasureIT software (Fig. 3b). The presence of γ -alumina layers decreases the support roughness, evidencing the formation of a smooth surface, ready to deposit silica on the top of it (Fig. 3b and c). Three different characteristic morphologies in the membrane's cross-section can be observed (Fig. 3b); the first one, rough, attributed to ceramic support providing mechanical stability to silica membrane; the second one, smooth, assigned to γ -alumina layer deposited on the top of ceramic support; and the last one, observed as a bright line in the outer size of the membrane, associated with

silica selective membrane layer deposited over the γ -alumina. The presence of silica on the intermediate γ -alumina layer was confirmed by X-ray EDS studies. However, the quantification of its layer thickness was impossible due to the low intensity of silicon on EDS spectra and the difficulty to establish clearly the limit between γ -alumina and silica layer, as it could be seen in Fig. 3c. It is not surprising considering the visible difference between the appreciable thickness of γ -Al₂O₃ layer (4 μ m) and that of silica (Fig. 3b).

The powder silica xerogel calcined at 400 °C is characterized with a narrow pore size distribution, with a maximum at 17 Å, which correspond to microporous material. Pore volume, porosity, and specific surface area of silica xerogel are 0.2686 cm³ g⁻¹, 37%, and 518 m² g⁻¹, respectively.

Table 3
Number of permeation model parameters to be fitted

Model	Parameters	Numbers of parameters	Total for n components
Fick's law	D_{ij_0} ; E_d	2	$2 \times n$
Solution–diffusion	P_{ij_0} ; E_d	2	$2 \times n$

Table 4

Selectivity and PSI values for acetic acid/isoamyl alcohol/isoamyl acetate mixture pervaporation using the ceramic membrane synthesized

Temperature (°C)	Selectivity		PSI	
	Water	Others	Water	Others
40	155.52	0.0065	170.41	0.00069
50	256.17	0.0043	257.03	0.00027
60	315.47	0.0033	295.58	0.00027

3.2. Permeation models correlation

First, selectivity and PSI values were determined. The PSI parameter can be used to identify optimal operation points and calculated from the fitted permeation model for industrial scale module design. It was calculated as the product of selectivity and flux.

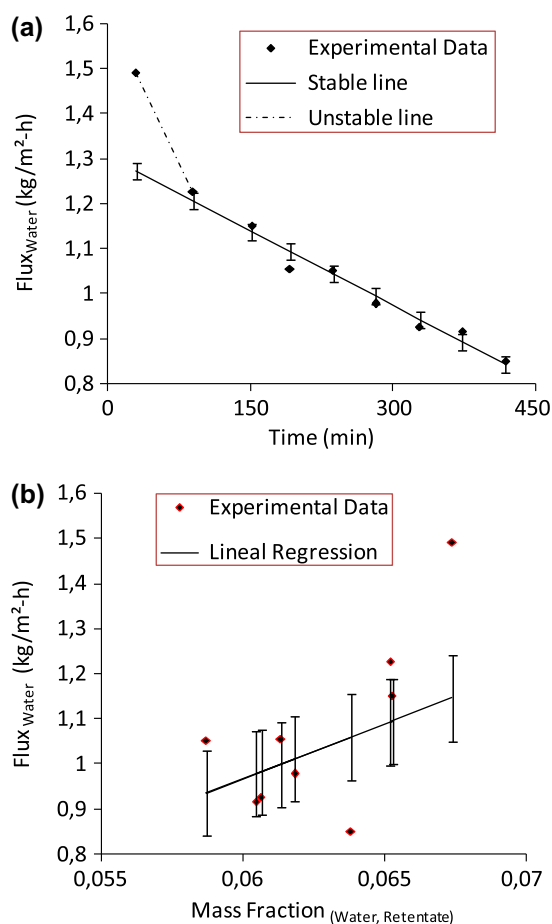


Fig. 4. (a) Flux of water vs. time, two distinctive slopes are identified, for instability period and for stable state. (b) Flux of water vs. water mass fraction in retentate. Bars show confidence interval of the regression.

Table 3 presents the number of permeation model parameters to be fitted. Calculated values of selectivity and PSI for synthesized silica membrane are presented in Table 4.

As an example of data processing, Fig. 4(a) shows the experimental values of water flux vs. time and the corresponding states of mass transport phenomena in the membrane. An unstable period is followed by a stable period in which the plot has a constant slope. Flux and corresponding retentate concentration is shown in Fig. 4(b).

As far as we know, no data are available in the open literature for comparison. However, pervaporation performance of the tested silica membrane in the dehydration of ethanol (6 wt.% of water) was also verified and was better than polymeric as well as ceramic commercially available tubular membranes for dewatering of organics [37,38]. The obtained values of total flux ($0.417 \text{ kg m}^{-2} \text{ h}^{-1}$) and water selectivity (207) are one of the highest reported in the literature [39,40].

Table 5 shows optimal values for the correlated parameters of each permeation model. The obtained values have physical meaning [41,42], even though for some parameters its calculated uncertainty (not shown) is of the same order of magnitude as the parameter itself. In the retentate concentration range tested, membrane retains its preferential affinity for water, independent of changes in composition during the experiment. The PSI values show the same trend observed for selectivity.

Mean error (with confidence interval) in flux predictions using the adjusted models are presented in Table 6 (calculated as $\text{Error} = \text{average} \pm \sigma^2$). To illustrate models predictions (using correlated parameters from Table 5), experimental vs. calculated flux parity plot are depicted in Fig. 5.

The comparison of the three adjusted permeation models (through their respective residual deviation from experimental data) defined that the model with the lowest deviation corresponds to the classical Fick's law (0.0744). However, this model does not incorpo-

Table 5
Values for correlated parameters in permeation models tested

	Classic Fick equations (5) and (6)		Thermodynamic Fick equation (7)		Solution–diffusion equation (8)	
	D_{ij_0} (m/h)	E_d (kJ/mol)	D_{ij_0} (m/h)	E_d (kJ/mol)	P_{ij_0} (kg/m-h)	E_d (kJ/mol)
Acid	6.6228	26.5307	1.92E–01	21.857	6.15E–12	1,498.47
Alcohol	6.44E–05	3.37E–13	9.63E–06	7.86E–13	5.58E–06	135,645.6
Ester	29.2678	24,176.68	9.86E–02	29.950	4.853031	58,947.05
Water	22.6027	18.8886	0.112	7.811	2.31E–10	1,344.564

Table 6
Mean error deviation between experimental and calculated flux values for different permeation models correlated

Model	Compound	Average error	σ^2	Residual error ^a
Classic Fick's law	Acid	0.0146	0.0066	0.0744
	Alcohol	0.0071	0.0039	
	Ester	0.0056	0.0018	
	Water	0.0679	0.0369	
	Total ^b	0.0238	0.0317	
Thermodynamic Fick's law	Acid	0.0175	0.0069	0.0847
	Alcohol	0.0080	0.0069	
	Ester	0.0006	0.0006	
	Water	0.0716	0.0400	
	Total	0.0244	0.0345	
Solution–diffusion	Acid	0.0169	0.0108	0.1080
	Alcohol	0.0114	0.0084	
	Ester	0.0056	0.0018	
	Water	0.0928	0.0551	
	Total	0.0317	0.0345	

^aMeasured as $\Sigma(J_{\text{Cal}} - J_{\text{Exp}})^2$, flux in $\text{kg}/\text{m}^2\text{h}$.

^bConsidering the entire data-set as the average of $(J_{\text{Cal}} - J_{\text{Exp}})$.

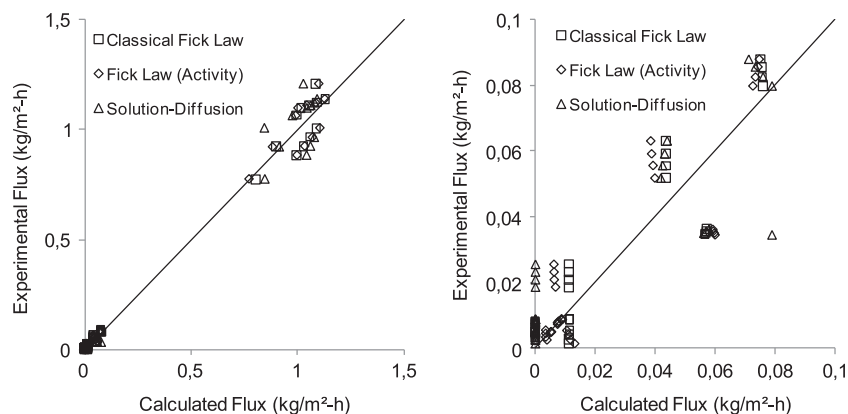


Fig. 5. Experimental results vs. permeation model predictions for water flux in a parity plot. Right figure is an amplification of the left one.

rate permeate pressure, a fundamental variable to rigorously describe pervaporation process. Therefore, it is considered to choose thermodynamic Fick model (0.0847) as the most suitable, which also includes retentate liquid phase nonideality.

4. Conclusions

Synthesis, characterization, and evaluation of a xerogel type hydrophilic ceramic membrane were conducted for water separation in acetic acid/isoamyl alcohol/isoamyl acetate/water mixtures. Conventional drawbacks in the evaluation of membrane performance for reactive mixtures pervaporation studies led to an alternative and suitable experimental procedure and method for experimental data analysis. With the proposed methodology, experimental flux data can be used to fit the corresponding parameters for different permeation models. In the composition range at which the experiments were conducted, the tested ceramic membrane retains its preferential affinity for water permeation. The PSI values exhibit the same trend observed for selectivity and its predictions using the correlated permeation model will identify optimal operating points for industrial scale module design. The comparison of the three adjusted permeation models (through their respective residual deviation) allows us to choose the thermodynamic Fick model (0.0847) as a reliable permeation model that will be used for the process design and simulation.

Acknowledgments

ECOPETROL-COLCIENCIAS-UNIVERSIDAD NACIONAL DE COLOMBIA, SEDE MANIZALES are gratefully acknowledged for financial support (Project number: 1119-490-26022). Miguel Duque-Bernal and Ana-Catalina Duque-Salazar are also acknowledged for their experimental work.

References

- [1] Ministerio de Minas y Energía. Republica de Colombia. Decreto 1135, 2009 (enacted). Available from: <http://www.minminas.gov.co/minminas/downloads/archivosSoporteRevistas/4783.pdf>.
- [2] Z. Küçükcü, K. Ceylan, Potential utilization of fusel oil: A kinetic approach for production of fusel oil esters through chemical reaction, *Turk. J. Chem.* 22 (1998) 289–300.
- [3] M. Yilmaztekin, H. Erten, T. Cabaroğlu, Enhanced production of isoamyl acetate from beet molasses with addition of fusel oil by *Williopsis saturnus* var. *saturnus*, *Food Chem.* (2009) 290–294.
- [4] F. Bi, S. Iqbal, A. Ali, M. Arman, M. UHassan, Synthesis of isoamyl acetate of isoamyl alcohol obtained from fusel oil using immobilized *Candida antarctica* lipase, *J. Chem. Soc. Pak.* 31 (2009) 485–491.
- [5] M. Duque Bernal, Esterificación de Ácido Acético con Alcohol Isoamílico: Un Estudio Cinético Usando Amberlite IR-120, M. Sc. Thesis, Universidad Nacional de Colombia Sede Manizales, 2011.
- [6] A. Wyczesany, Chemical equilibrium constants in esterification of acetic acid with C1–C5 alcohols in the liquid phase, *Chem. Process Eng.* 30 (2009) 243–265.
- [7] Y. Seong, B.P. Lim, Design issues of pervaporation membrane reactors for esterification, *Chem. Eng. Sci.* 57 (2002) 4933–4946.
- [8] W. Kujawski, Application of pervaporation and vapor permeation in environmental protection, *Polish J. Environ. Stud.* 9 (2000) 13–17.
- [9] M. Duque Bernal, J.D. Quintero Arias, J. Fontalvo, M.Á. Gómez García, Elementos para la intensificación del proceso de producción de acetato de amilo utilizando tecnología de membranas, Medellín: XXV Congreso colombiano de ingeniería química, 2009.
- [10] J. Fontalvo, M.Á. Gómez-García, Intensificación de Procesos Utilizando Tecnología de Membrana [Process Intensification by Membrane Technologies], 1st ed., Universidad Nacional de Colombia, Manizales, 2010.
- [11] Kirk-Othmer, Encyclopedia of Chemical Technology, John Wiley & Sons, New York, NY, 1998.
- [12] R. Smith, Chemical Process Design and Integration, John Wiley & Sons, Chichester, 2005.
- [13] R. Krishna, J.A. Wesselingh, The Maxwell-Stefan approach to mass transfer, *Chem. Eng. Sci.* 52 (1997) 861–911.
- [14] Fahmy, Membrane Processes for the Dehydration of Organic Compounds, Ph.D. Thesis, Germany, Hannover University, 2002.
- [15] J.D. Seader, E.J. Henley, Separation Process Principles, John Wiley & Sons, Hoboken, NJ, 2006.
- [16] Y. Huang, J. Fu, Y. Zhou, X. Huang, X. Tang, Pervaporation performance of trifluoroethoxy substituting polyphosphazene membrane for different organic compounds aqueous solutions, *Desalin. Water Treat.* 24 (2010) 210–219.
- [17] T. Peters, J. Fontalvo, M. Vorstman, N. Benes, R. Dam, Z. Vroon, Hollow fiber microporous silica membranes for gas separation and pervaporation. Synthesis performance and stability, *J. Membr. Sci.* 248 (2005) 73–80.
- [18] Z. Yun, T. Zhangfa, L. Kun, F. Xianshe, Modeling of esterification in a batch reactor coupled with pervaporation for production of n-butyl acetate, *Chin. J. Catal.* 31 (2010) 999–1005.
- [19] R. Krupiczka, Z. Koszorz, Activity based model of the hybrid process of an esterification reaction coupled with pervaporation, *Sep. Purif. Technol.* 16 (1999) 55–59.
- [20] Z. Xu, Y. Shi, Study on the coupling process of pervaporation and chemical reaction(I): Theoretical analysis, *Membr. Sci. Technol.* 16 (1996) 58.
- [21] A.C. Duque Salazar, Development of Silica Containing Materials for the Adsorption of Organic Compounds, M.Sc. Thesis, Universidad Nacional de Colombia, Manizales, 2011.
- [22] R.S.A. de Lange, J.H.A. Hekink, H.K. Keizer, A.J. Burggraaf, Formation and characterization of supported microporous ceramic membranes prepared by sol-gel modification techniques, *J. Membr. Sci.* 99 (1995) 57–75.
- [23] R.M. de Vos, H. Verweij, Hydrophobic silica membranes for gas separation, *J. Membr. Sci.* 158 (1999) 277–288.
- [24] K. Czarnobaj, Preparation and characterization of silica xerogels as carriers for drugs, *Drug Delivery* 15 (2008) 485–492.
- [25] W. Verkerk, Application of Silica Membranes in Separations and Hybrid Reactor Systems. Ph.D. Thesis, Technical University of Eindhoven, 2003.
- [26] H. Brüschke, Industrial application of membrane separation processes, *Pure Appl. Chem.* 67 (1995) 993–1002.
- [27] M. Wesslein, A. Heintz, R. Lichtenthaler, Pervaporation of liquid mixtures through poly(vinyl alcohol) (PVA) membranes. I. Study of water containing binary systems with complete and partial miscibility, *J. Membr. Sci.* 51 (1990) 169–179.
- [28] C.C. Coterillo, A.M. Mendia, I.O. Uribe, Pervaporation and gas separation using microporous membranes, *Membr. Sci. Technol.* (2008) 217–253.
- [29] H. Kasaini, L. Malherbe, R. Everson, K. Keizer, H. Neomagus, A predictive model for permeation flux in a membrane reactor: Aspects of esterification, *Sep. Sci. Technol.* (2005) 433–452.

- [30] P. Englezos, N. Kalogerakis, *Applied Parameter Estimation for Chemical Engineers*, Marcel Dekker, New York, NY, 2001.
- [31] C.M. Bishop, M. Svensén, *Pattern Recognition and Machine Learning*, Springer, New York, NY, 2006.
- [32] A.C. Duque-Salazar, M.A. Gómez García, J. Fontalvo, M. Jedrzejczyk, J.M. Rynkowski, I. Dobrosz-Gómez, Ethanol dehydration by pervaporation using microporous silica membranes. *Desalin. Water Treat.*, DOI - 10.1080/19443994.2012.728053
- [33] T. Takei, Infrared spectra of geminal and novel triple hydroxyl groups on silica surface, *Colloids Surf. A: Physicochem. Eng. Aspects* 150(1–3) (1999) 77–84.
- [34] R. Al-Oweini, H. El-Rassy, Synthesis and characterization by FTIR spectroscopy of silica aerogels prepared using several Si(OR)₄ and R'Si(OR)₃ precursors, *J. Mol. Struct.* 919(1–3) (2009) 140–140.
- [35] G. Socrates, *Infrared and Raman Characteristic Group Frequencies. Tables and charts*, second ed., Wiley, Chichester, 1994.
- [36] B. Stuart, *Infrared Spectroscopy: Fundamentals and Applications*. Wiley, Chichester, 2004.
- [37] H.M. van Veen, Y.C. van Delft, C.W.R. Engelen, P.P.A.C. Pex, Dewatering of organics by pervaporation with silica membranes, *Sep. Purif. Technol.* 2223 (2001) 361–366.
- [38] I. Ortiz, D. Gorri, C. Casado, A. Urriaga, Modelling of the pervaporative flux through hydrophilic membranes, *J. Chem. Technol. Biotechnol.* 80 (2005) 397–405.
- [39] K. Sakaki, H. Habe, H. Negishi, T. Ikegami, Pervaporation of aqueous dilute 1-butanol, 2-propanol, ethanol and acetone using a tubular silicalite membrane, *Desalin. Water Treat.* 34 (2011) 290–294.
- [40] A. Hasanoglu, S. Dincer, Modelling of a pervaporation membrane reactor during esterification reaction coupled with separation to produce ethyl acetate, *Desalin. Water Treat.* 35 (2011) 286–294.
- [41] A. Noworyta, M. Kubasiewicz-Ponitka, A. Kozio, Mass and heat transport resistance in pervaporation process, *Desalin. Water Treat.* 26 (2011) 226–235.
- [42] M. Staniszewski, W. Kujawski, Modeling of the kinetics of pervaporative recovery of ethanol from fermented broth with the use of the solution-diffusion theory, *Desalin. Water Treat.* 14 (2010) 185–191.